A Dynamical Systems Approach to a Bianchi Type I Viscous Magnetohydrodynamic Model

Ikjyot Singh Kohli*
York University - Department of Physics and Astronomy

Michael C. Haslam†
York University - Department of Mathematics and Statistics

(Dated: April 1, 2013)

We use the expansion-normalized variables approach to study the dynamics of a non-tilted Bianchi Type I cosmological model with both a pure, homogeneous source-free magnetic field and viscous fluid with both bulk and shear viscous effects, employing the ideal magnetohydrodynamic approximation. The dynamical system is then studied in detail through a fixed-point analysis which determines the local sink and source behaviour in combination with standard dynamical system theory and numerical experiments that give a very good indication of the asymptotic behaviour of the system. It is further shown that for certain values of the bulk and shear viscosity and equation of state parameters, the model isotropizes at late times.

I. INTRODUCTION

The current standard model of cosmology based on the Friedmann-LeMaitre-Robertson-Walker metric assumes that the universe to a very high degree is spatially homogeneous and isotropic, which implies the existence of a perfect fluid matter distribution. However, if one wishes to formulate a cosmological model of the early universe, including anisotropic terms in the energy-momentum tensor is necessary.

Viscous models have become of general interest in early-universe cosmologies largely in two contexts. Grøn and Hervik (Chapter 13, [1]) discuss these in some detail. The first relates through the idea of inflation through bulk viscosity. In models where bulk viscous terms are permitted to dominate, they drive the universe into a de Sitter-like state. Because of these processes, the models isotropize indirectly through the massive expansion. Shear viscosity is found to play an important role in universe models with dissipative fluids. The dissipative processes that result from shear viscous terms are thought to be highly effective during the early stages of the universe. In particular, neutrino viscosity is considered to be one of the most important factors in the isotropization of our universe.

Magnetic fields have also been thought to play a major role in the early universe, as it is well-known that after inflation, the early universe was a good conductor, even though the number density of free electrons dropped dramatically during recombination, its residual value was enough to maintain high conductivity in baryonic matter. As a result, cosmic magnetic fields have remained frozen into the expanding baryonic fluid during most of their evolution (Page 115, [2]). One can then analyze the magnetic effects on the dynamics of the early universe through the ideal magnetohydrodynamics (hereafter, referred to as MHD), in which the magnetic field source is considered to be a perfect conductor, such that the energy momentum tensor is that for an ordinary magnetic field.

Hughston and Jacobs [3] showed the in the case of a pure magnetic field, only Bianchi Types I, II, VI($h = -1$) (which is the same as Type III), and VII ($h = 0$) admit field components, whereas Types IV, V, VI ($h = -1$), VII ($h \neq 0$), VIII, and IX admit no field components. These results led to a number of papers of Bianchi models with a perfect-fluid magnetic field source.

With respect to the dynamical systems approach applied to the latter, which is what we are interested in studying in this work, LeBlanc studied Bianchi Type II magnetic cosmologies in which he provided an analysis on the future and past asymptotic states of the resulting dynamical system [4]. LeBlanc also studied the asymptotic states of magnetic perfect-fluid Bianchi Type I cosmologies [5]. Using phase plane analysis techniques, Collins studied the behaviour of a class of perfect-fluid anisotropic cosmological models, and established a correspondence between magnetic models of Bianchi Type I and perfect fluid models of Bianchi Type II [6]. In addition, LeBlanc, Kerr, and Wainwright studied the asymptotic states of magnetic Bianchi Type VI cosmologies. In their work, they showed that there is a finite probability that an arbitrarily selected model will be close to isotropy during some time interval in its evolution [7]. We should note that Barrow, Maartens, and Tsagas did significant work in the reformulation of a $1 + 3$ covariant

*Electronic address: isk@yorku.ca
†Electronic address: mchaslam@mathstat.yorku.ca

description of the magnetohydrodynamic equations that has provided further understanding and clarity on the role of large-vale electromagnetic fields in the perturbed Friedmann-LeMaitre-Robertson-Walker models [8].

Viscous MHD Bianchi models, which are of interest to us have been presented in the literature on a number of occasions. van Leeuwen and Salvati studied the dynamics of general Bianchi class A models containing a magneto-viscous fluid and a large-scale magnetic field [9]. Banerjee and Sanyal presented some exact solutions of Bianchi Types I and III cosmological models consisting of a viscous fluid and axial magnetic field [10]. Benton and Tupper studied Bianchi Type I models with a "powers-of-t" metric under the influence of a viscous fluid with a magnetic field [11]. Salvati, Schelling, and van Leeuwen numerically analyzed the evolution of the Bianchi type I universe with a viscous fluid and large-scale magnetic field [12]. Ribeiro and Sanyal studied a Bianchi Type VI_0 viscous fluid cosmology with an axial magnetic field in which they obtained exact solutions to the Einstein field equations assuming linear relations among the square root of matter density and the shear and expansion scalars [13]. van Leeuwen, Miedema, and Wiersma proved that a nonrotating Bianchi model of class A containing a viscous fluid and magnetic field can only be of Type I or IV_0 [14]. Pradhan and Pandey studied the Bianchi Type I model with a bulk viscous fluid in addition to a varying cosmological constant [15]. Pradhan and Singh studied the Bianchi Type I model in the presence of a magnetic field and shear and bulk viscosity, but assumed that the shear tensor was proportional to the expansion tensor [16]. Bali and Anjali studied a Bianchi Type I magnetized fluid model with a bulk viscous string dust fluid, in which they compared their results in the presence and absence of large-scale magnetic fields [17].

We wish to study a Bianchi Type I non-tilted viscous magnetohydrodynamic model, but using the Hubble-normalized dynamical systems approach based upon the theory of orthonormal frames pioneered by Ellis and MacCallum [18], which reduces the Einstein field equations, a coupled set of ten hyperbolic nonlinear partial differential equations to a system of autonomous nonlinear first-order ordinary differential equations. Such an approach has not been taken in the existing literature, which we believe will add valuable information to this already rich, but ever-expanding field. The advantage to using this approach is that one can obtain a very deep understanding of the evolution of these models at early times (near the initial singularity), at late times, and at intermediate times. This is mainly accomplished through a fixed-point analysis of the dynamical system where connections are then made with the global dynamics through sophisticated numerical experiments. Throughout, we assume that the signature of the metric tensor is $(-,+,+,+)$, and the use of *geometrized units*, where $G = c = 1$.

II. THE MATTER SOURCES

For a viscous fluid magnetic cosmological model there are two contributions to the total energy-momentum tensor: the viscous contributions due to the shear and bulk viscosity and the magnetic field contribution. We will assume for simplicity that our fluid has negligible heat conduction, such that the heat flux vector vanishes. Then, the viscous fluid energy-momentum tensor is given by

$$\mathcal{V}_{ab} = (\mu_f + p_f)u_a u_b + g_{ab}p_f - 3\xi H h_{ab} - 2\eta\sigma_{ab}, \tag{1}$$

where μ_f, p_f, and σ_{ab} denote the energy density, pressure, and shear tensor due to the fluid, ξ and η denote the bulk and shear viscosity coefficients of the fluid, H denotes the Hubble parameter, and $h_{ab} \equiv u_a u_b + g_{ab}$ denotes the projection tensor corresponding to the aforementioned metric signature. A detailed derivation of Eq. (1) can be found in [19].

Following the arguments given on Pages 6 and 14 in [20], we note that the energy-momentum tensor for an electromagnetic field is given by

$$\mathcal{T}_{ab} = \frac{1}{2}u_a u_b(E^2 + B^2) + 2u_{(a}n^{cgd}_{b)}u_c E_g B_d - E_a E_b - B_a B_b + \frac{1}{2}h_{ab}\left(E^2 + B^2\right), \tag{2}$$

where n^{abcd} is the standard skew pseudo tensor, and E_a and B_a are the electric and magnetic field three-vectors respectively. Note that in an orthonormal frame where $g_{ab} = n_{ab} = diag(-1,1,1,1)$, the E^2 and B^2 terms in Eq. (2), take the form $E^2 \equiv E^a E_a = E_1^2 + E_2^2 + E_3^2$, and $B^2 \equiv B^a B_a = B_1^2 + B_2^2 + B_3^2$. In addition,since we are assuming that the cosmological model is non-tilted, in both Eqs. (1) and (2), u_a is the four-velocity of a comoving observer such that $u^a = (1,0,0,0)$.

For our purposes, we are to consider the ideal MHD approximation, where we assume that the early universe behaves as a *perfect* conductor. Then, the electric field, which is inversely proportional to the conductivity approaches zero, even if there is a current flowing. In other words, we are assuming that after recombination, the universe is such a good conductor that the cosmic electric fields required to drive current in it is negligible. Taking these arguments into account, Eq. (2) takes the form

$$\mathcal{T}_{Bab} = \frac{1}{2}u_a u_b\left(B^2\right) - B_a B_b + \frac{1}{2}h_{ab}B^2. \tag{3}$$

The total energy-momentum tensor, denoted $\mathbb{T}_{ab}$, for our cosmological model is then

$$\mathbb{T}_{ab} = \mathcal{V}_{ab} + \mathcal{T}_{Bab}, \tag{4}$$

where $\mathcal{V}_{ab}$ is given by Eq. (1), and $\mathcal{T}_{Bab}$ is given by Eq. (3).

In order to formulation the evolution equations for our model, we will be required to know the total energy density, total pressure, and total anisotropic stress from Eq. (4), which we will respectively denote by $\tilde{\mu}, \tilde{p}$, and $\tilde{\pi}_{ab}$. Using the definitions

$$\tilde{\mu} = \mathbb{T}_{ab}u^a u^b, \quad \tilde{p} = \frac{1}{3}h^{ab}\mathbb{T}_{ab}, \quad \tilde{\pi}_{ab} = h^c_a h^d_b \mathbb{T}_{cd} - \tilde{p}h_{ab}, \tag{5}$$

we find that

$$\tilde{\mu} = \mu_f + \frac{1}{2}\left(B_1^2 + B_2^2 + B_3^2\right), \tag{6}$$

$$\tilde{p} = w\mu_f - 3\xi H + \frac{1}{6}\left(B_1^2 + B_2^2 + B_3^2\right), \tag{7}$$

and

$$\tilde{\pi}_{ab} = -2\eta\sigma_{ab} - B_a B_b + \frac{1}{3}h_{ab}\left(B_1^2 + B_2^2 + B_3^2\right). \tag{8}$$

Note that in Eq. (7), we made use of the assumption that the fluid obeys the barotropic equation of state, $p_f = w\mu_f$, where $-1 \leq w \leq 1$.

Since we are dealing with expansion-normalized variables, we will re-write Eqs. (6) - (8) using the definitions [21]:

$$\tilde{\Omega} = \frac{\tilde{\mu}}{3H^2}, \quad \tilde{P} = \frac{\tilde{p}}{3H^2}, \quad \tilde{\Pi}_{ab} = \frac{\tilde{\pi}_{ab}}{H^2}. \tag{9}$$

We will also define the expansion-normalized magnetic field vector as

$$\mathcal{B}_a = \frac{B_a}{3H}. \tag{10}$$

According to the definitions in Eq. (9), the expansion-normalized source variables take the form:

$$\tilde{\Omega} = \Omega_f + \frac{3}{2}\left(\mathcal{B}_1^2 + \mathcal{B}_2^2 + \mathcal{B}_3^2\right), \tag{11}$$

$$\tilde{P} = w\Omega_f - 3\xi_0 + \frac{1}{2}\left(\mathcal{B}_1^2 + \mathcal{B}_2^2 + \mathcal{B}_3^2\right), \tag{12}$$

and

$$\tilde{\Pi}_{ab} = -2\eta_0\Sigma_{ab} - 9\mathcal{B}_a\mathcal{B}_b + 3\delta_{ab}\left(\mathcal{B}_1^2 + \mathcal{B}_2^2 + \mathcal{B}_3^2\right). \tag{13}$$

In Eqs. (12) and (13), ξ_0 and η_0 are the expansion-normalized bulk and shear viscosity coefficients, and are defined according to

$$\frac{\xi}{H} = 3\xi_0, \quad \frac{\eta}{H} = 3\eta_0. \tag{14}$$

Throughout this paper, we will assume that both ξ_0 and η_0 are *non-negative constants*. In addition, in Eq. (13), Σ_{ab} is the expansion-normalized shear tensor defined according to $\Sigma_{ab} = \sigma_{ab}/H$.

III. BIANCHI TYPE I UNIVERSE DYNAMICS

With the required energy-momentum tensor (Eq. (4)), and the expansion-normalized source variables (Eqs. (11) - (13)) in hand, we will now derive the Bianchi Type I dynamical equations. The general evolution equations for any Bianchi type have already been derived in [21] and [22], and we will simply make use of their results in this section.

The general evolution equations in the expansion-normalized variables using our notation are:

$$\begin{aligned}
\Sigma'_{ij} &= -(2-q)\Sigma_{ij} + 2\epsilon^{km}_{(i}\Sigma_{j)k}R_m - \mathcal{S}_{ij} + \tilde{\Pi}_{ij} \\
N'_{ij} &= qN_{ij} + 2\Sigma^k_{(i}N_{j)k} + 2\epsilon^{km}_{(i}N_{j)k}R_m \\
A'_i &= qA_i - \Sigma^j_i A_j + \epsilon^{km}_i A_k R_m \\
\tilde{\Omega}' &= (2q-1)\tilde{\Omega} - 3\tilde{P} - \frac{1}{3}\Sigma^j_i\tilde{\Pi}^i_j + \frac{2}{3}A_iQ^i \\
Q'_i &= 2(q-1)Q_i - \Sigma^j_iQ_j - \epsilon^{km}_iR_kQ_m + 3A^j\tilde{\Pi}_{ij} + \epsilon^{km}_iN^j_k\tilde{\Pi}_{jm}.
\end{aligned} \tag{15}$$

These equations are subject to the constraints

$$\begin{aligned}
N^j_iA_j &= 0 \\
\tilde{\Omega} &= 1 - \Sigma^2 - K \\
Q_i &= 3\Sigma^k_iA_k - \epsilon^{km}_i\Sigma^j_kN_{jm}.
\end{aligned} \tag{16}$$

As in Eq. (9), we have made use of the following notation:

$$\left(\Sigma_{ij}, R^i, N^{ij}, A_i\right) = \frac{1}{H}\left(\sigma_{ij}, \Omega^i, n^{ij}, a_i\right), \quad \left(\tilde{\Omega}, \tilde{P}, Q_i, \tilde{\Pi}_{ij}\right) = \frac{1}{3H^2}\left(\tilde{\mu}, \tilde{p}, q_i, \tilde{\pi}_{ij}\right). \tag{17}$$

In the expansion-normalized approach, Σ_{ab} denotes the kinematic shear tensor, and describes the anisotropy in the Hubble flow, A_i and N^{ij} describe the spatial curvature, while Ω^i describes the relative orientation of the shear and spatial curvature eigenframes.

The dynamical system (15) evolves according to a dimensionless time variable, τ such that

$$\frac{dt}{d\tau} = \frac{1}{H}, \tag{18}$$

where H is the Hubble parameter. The deceleration parameter q is very important in the expansion-normalized approach, and through the evolution equation for H

$$H' = -(1+q)H, \tag{19}$$

Eq. (1.90) in [23], and using Eq. (17), one can show that q is defined as

$$\begin{aligned}
q &\equiv 2\Sigma^2 + \frac{1}{2}\left(\tilde{\Omega} + 3\tilde{P}\right) \\
&= 2\Sigma^2 + \Omega_f\left(\frac{1}{2} + \frac{3w}{2}\right) - \frac{9}{2}\xi_0 + \frac{3}{2}\left(\mathcal{B}^2_1 + \mathcal{B}^2_2 + \mathcal{B}^2_3\right),
\end{aligned} \tag{20}$$

where $2\Sigma^2 \equiv \frac{1}{3}\left(\Sigma_{ab}\Sigma^{ab}\right)$.

In the case of a magnetic field source, one must also include an evolution equation for the magnetic field, which is the orthonormal frame analog of the standard Maxwell's equation. According to Eq. (71) in [24], Eq. (2.4) in [7], and Eqs. (10), (17), (18), and (19) above, the magnetic field evolution is given by

$$\mathcal{B}'_a = \mathcal{B}_a\left(-1+q\right) + \Sigma_{ab}\mathcal{B}^b + \epsilon_{abv}R^v\mathcal{B}^b \tag{21}$$

The Bianchi Type I model is a flat anisotropic model and is Abelian, and therefore has the property that

$$A^i = 0, \quad N_{11} = N_{22} = N_{33} = 0. \tag{22}$$

For convenience, we introduce the notation

$$\Sigma_+ = \frac{1}{2}\left(\Sigma_{22} + \Sigma_{33}\right), \quad \Sigma_- = \frac{1}{2\sqrt{3}}\left(\Sigma_{22} - \Sigma_{33}\right), \tag{23}$$

such that $\Sigma^2 = \Sigma_+^2 + \Sigma_-^2$. In the evolution equations (15), the expansion-normalized angular velocity variables R_a can be found from the non-diagonal shear equations, $\Sigma_{12}', \Sigma_{23}'$, and Σ_{13}'. From these equations, we get that

$$R_1 = -\frac{3\sqrt{3}\mathcal{B}_2\mathcal{B}_3}{2\Sigma_-}, \quad R_2 = \frac{9\mathcal{B}_1\mathcal{B}_3}{\sqrt{3}\Sigma_- - 3\Sigma_+}, \quad R_3 = \frac{9\mathcal{B}_1\mathcal{B}_2}{\sqrt{3}\Sigma_- + 3\Sigma_+}. \tag{24}$$

To avoid situations where $\sqrt{3}\Sigma_- - 3\Sigma_+ = 0$ or $\sqrt{3}\Sigma_- + 3\Sigma_+ = 0$, we will set $\mathcal{B}_1 = \mathcal{B}_3 = 0$, and keep $\mathcal{B}_2 \neq 0$. Then, $R_1 = R_2 = R_3 = 0$, and according to Eqs. (24), (23), (22), and (20), the evolution equations (15) and the constraint equations (16) become:

$$\Sigma_+' = -\frac{3}{2}\mathcal{B}_2^2 + \Sigma_+ \left[q - 2\left(1 + \eta_0\right)\right], \tag{25}$$

$$\Sigma_-' = -\frac{3\sqrt{3}}{2}\mathcal{B}_2^2 + \Sigma_- \left[q - 2\left(1 + \eta_0\right)\right], \tag{26}$$

$$\mathcal{B}_2' = \mathcal{B}_2\left(-1 + q + \sqrt{3}\Sigma_- + \Sigma_+\right), \tag{27}$$

$$\Omega_f = 1 - \frac{3}{2}\mathcal{B}_2^2 - \Sigma_-^2 - \Sigma_+^2 \geq 0, \tag{28}$$

where

$$q = 2\left(\Sigma_+^2 + \Sigma_-^2\right) + \Omega_f\left(\frac{1}{2} + \frac{3w}{2}\right) - \frac{9}{2}\xi_0 + \frac{3}{2}\mathcal{B}_2^2, \quad -1 \leq w \leq 1, \quad \xi_0 \geq 0, \quad \eta_0 \geq 0. \tag{29}$$

The auxiliary equation, $\tilde{\Omega}'$ in (15), after some algebra, takes the form

$$\Omega_f' = \Omega_f\left(2q - 1 - 3w\right) + 4\eta_0\left(\Sigma_+^2 + \Sigma_-^2\right) + 9\xi_0. \tag{30}$$

IV. A FIXED POINT ANALYSIS

In this section, we consider the local stability of the equilibrium points of the system (25)-(27). The first thing to note is that the dynamical system Eqs. (25)- (27) can be written as

$$\mathbf{x}' = \mathbf{f}(\mathbf{x}), \tag{31}$$

where $\mathbf{x} = [\Sigma_+, \Sigma_-, \mathcal{B}_2] \in \mathbf{R}^3$, and $\mathbf{f}(\mathbf{x})$ denotes the right-hand-side of the dynamical system.

The state space of the system is the subset of $\mathbb{R}^3$ defined by the inequality in Eq. (28), which is equivalent to

$$\Sigma_+^2 + \Sigma_-^2 + \frac{3}{2}\mathcal{B}_2^2 \leq 1, \tag{32}$$

so the state space is clearly bounded. This inequality also is a constraint for the initial conditions of the dynamical system.

There is only one symmetry of the dynamical system and it is given by

$$[\Sigma_+, \Sigma_-, \mathcal{B}_2] \to [\Sigma_+, \Sigma_-, -\mathcal{B}_2], \tag{33}$$

so the system is invariant with respect to spatial inversions in the function $\mathcal{B}_2$, and we can therefore take $\mathcal{B}_2 \geq 0$.

The critical points are points $\mathbf{x} = \mathbf{a}$ that simultaneously satisfy

$$\mathbf{f}(\mathbf{a}) = 0, \tag{34}$$

where $\mathbf{f}$ denotes the right-hand-side of the system (25)-(27). The local stability is determined by linearizing this system at $\mathbf{x} = \mathbf{a}$, which leads to the relationship $\mathbf{x}' = D\mathbf{f}(\mathbf{a})\mathbf{x}$. The stability of the system is then determined by finding the eigenvalues and eigenvectors of the derivative matrix $D\mathbf{f}(\mathbf{a})$. The restrictions on the parameters w, ξ_0, and η_0 are given by physically realistic limitations. Namely, we take the expansion-normalized viscosity coefficients ξ_0, η_0 to be nonnegative constants. Any combinations of these parameters must additionally satisfy $\Omega_f \geq 0$, $\Sigma_+ \in \mathbb{R}, \Sigma_- \in \mathbb{R}$, and $\mathcal{B}_2 \geq 0 \in \mathbb{R}$. In the work that follows, we will denote eigenvalues of the dynamical system by λ_i, where $i = 1, 2, 3, ...$

A. Equilibrium Point 1

$$\begin{aligned}\Sigma_+ &= \frac{1+2\eta_0 - w(1+2\eta_0) + \sqrt{-(-1+w)\left(9+4\eta_0-12\eta_0^2+3w\left(-3+4\eta_0+4\eta_0^2\right)+36\xi_0\right)}}{4(-1+w)},\\ \Sigma_- &= \frac{-3-6\eta_0 + w(3+6\eta_0) + \sqrt{-(-1+w)\left(9+4\eta_0-12\eta_0^2+3w\left(-3+4\eta_0+4\eta_0^2\right)+36\xi_0\right)}}{4\sqrt{3}(-1+w)},\\ \mathcal{B}_2 &= 0. \end{aligned} \tag{35}$$

The cosmological parameters at this point take the form

$$\Omega_f = \frac{4\eta_0+9\xi_0}{3(-1+w)}, \quad q = 2\left(1+\eta_0\right), \quad \Sigma^2 = \frac{3-3w+4\eta_0+9\xi_0}{3-3w}, \tag{36}$$

where

$$-1 \leq w < 1, \quad \eta_0 = 0, \quad \xi_0 = 0. \tag{37}$$

With the restrictions (37), the equilibrium point (35) takes the form:

$$\Sigma_+ = \frac{1+3\sqrt{(-1+w)^2}-w}{4(-1+w)}, \quad \Sigma_- = \frac{\sqrt{3}\left(-1+\sqrt{(-1+w)^2}+w\right)}{4(-1+w)}, \quad \mathcal{B}_2 = 0. \tag{38}$$

In addition, the cosmological parameters (36) take the form:

$$\Omega_f = 0, \quad q = 2, \quad \Sigma^2 = 1, \quad -1 \leq w < 1, \tag{39}$$

therefore, this point represents that of a *Kasner circle*, and we will denote it by $\mathcal{K}$. The eigenvalues of the dynamical system at this point are

$$\lambda_1 = 0, \quad \lambda_2 = 3-3w, \quad \lambda_3 = \frac{3\left(-1+\sqrt{(-1+w)^2}+w\right)}{2(-1+w)}. \tag{40}$$

We therefore see that in the region $-1 \leq w < 1$, $\xi_0 = \eta_0 = 0$, $\mathcal{K}$ represents a local source, and can never be a local sink. We will subsequently denote the region defined by (37) as U(K).

B. Equilibrium Point 2

$$\Sigma_+ = 0, \quad \Sigma_- = 0, \quad \mathcal{B}_2 = 0. \tag{41}$$

The cosmological parameters at this point take the form

$$\Omega_f = 1, \quad q = \frac{1}{2}\left(1+3w-9\xi_0\right), \quad \Sigma^2 = 0. \tag{42}$$

Clearly, this point represents the *flat FLRW* universe, which we will denote by $\mathcal{F}$. The eigenvalues of the dynamical system at this point are given by

$$\lambda_1 = \frac{1}{2}(-1+3w-9\xi_0), \quad \lambda_2 = \lambda_3 = \frac{1}{2}(-3+3w-4\eta_0-9\xi_0), \tag{43}$$

where in Eqs. (42) and (43), $\eta_0 \geq 0$, $\xi_0 \geq 0$, and $-1 \leq w \leq 1$.

The point $\mathcal{F}$ represents a local sink if

$$\eta_0 \geq 0, \quad \xi_0 \geq 0, \quad -1 \leq w < \frac{1}{3}, \tag{44}$$

or

$$\eta_0 \geq 0, \quad \frac{1}{3} \leq w \leq 1, \quad \xi_0 > \frac{1}{9}\left(-1+3w\right). \tag{45}$$

In Fig. (1), we have denoted the region defined by (44) and (45) as $S1(F)$.

An important point to note is that $q=-1$ when $0 \leq \xi_0 \leq \frac{2}{3}$ and $w = 3\xi_0 - 1$, thus, the equilibrium point in the domain defined by these values of η_0, ξ_0 ,and w does not correspond to a self-similar solution. In particular, if one chooses $\xi_0 = 0$ such that $w=-1$, the corresponding model is locally the de Sitter solution [2].

The point $\mathcal{F}$ represents a saddle point if

$$\eta_0 = 0, \quad \frac{1}{3} < w < 1, \quad 0 \leq \xi_0 < \frac{1}{9}(-1+3w), \tag{46}$$

or

$$\eta_0 = 0, \quad w = 1, \quad 0 < \xi_0 < \frac{2}{9}, \tag{47}$$

or

$$\eta_0 > 0, \quad \frac{1}{3} < w \leq 1, \quad 0 \leq \xi_0 < \frac{1}{9}\left(-1+3w\right), \tag{48}$$

where in each case $\lambda_1 > 0$ and $\lambda_2 = \lambda_3 < 0$. We will subsequently denote the region defined by (46) - (48) as SA(F).

The point $\mathcal{F}$ can also represent a local source if

$$\eta_0 = 0, \quad w = 1, \quad \xi_0 = 0, \tag{49}$$

where in this case, $\lambda_1 > 0$ and $\lambda_2 = \lambda_3 = 0$. IWe will subsequently denote the region defined by Eq. (49) as U(F).

C. Equilibrium Point 3

We will denote this equilibrium point as $\mathcal{BI}_{\mathcal{MV}}$.

$$\Sigma_+ = -\frac{1}{16(5-6\eta_0+w(3+6\eta_0))}\left(35-52\eta_0+12\eta_0^2+9(w+2w\eta_0)^2+w\left(36+48\eta_0-48\eta_0^2\right)\right.$$
$$\left.+\sqrt{(5-6\eta_0+w(3+6\eta_0))^2\left(81-6w(3-2\eta_0)^2-28\eta_0+4\eta_0^2+9(w+2w\eta_0)^2+288\xi_0\right)}\right),$$

$$\Sigma_- = -\frac{1}{16(5-6\eta_0+w(3+6\eta_0))}\sqrt{3}\left(35-52\eta_0+12\eta_0^2+9(w+2w\eta_0)^2+w\left(36+48\eta_0-48\eta_0^2\right)\right.$$
$$\left.+\sqrt{(5-6\eta_0+w(3+6\eta_0))^2\left(81-6w(3-2\eta_0)^2-28\eta_0+4\eta_0^2+9(w+2w\eta_0)^2+288\xi_0\right)}\right),$$

$$\mathcal{B}_2 = \frac{1}{4\sqrt{3}}\left(\sqrt{\left(-51+12w(1-2\eta_0)^2+52\eta_0-12\eta_0^2-9(w+2w\eta_0)^2-144\xi_0\right.\right.$$
$$\left.\left.-\sqrt{(5-6\eta_0+w(3+6\eta_0))^2\left(81-6w(3-2\eta_0)^2-28\eta_0+4\eta_0^2+9(w+2w\eta_0)^2+288\xi_0\right)}\right)}\right). \tag{50}$$

The cosmological parameters at this point take the form

$$\Omega_f = -\frac{1}{16(5-6\eta_0+w(3+6\eta_0))}\left(-45+114\eta_0-92\eta_0^2+24\eta_0^3-12w(1-2\eta_0)^2(1+2\eta_0)+9w^2(1+2\eta_0)^3\right.$$
$$+\sqrt{(5-6\eta_0+w(3+6\eta_0))^2\left(81-6w(3-2\eta_0)^2-28\eta_0+4\eta_0^2+9(w+2w\eta_0)^2+288\xi_0\right)}$$
$$\left.+2\eta_0\sqrt{(5-6\eta_0+w(3+6\eta_0))^2\left(81-6w(3-2\eta_0)^2-28\eta_0+4\eta_0^2+9(w+2w\eta_0)^2+288\xi_0\right)}\right),$$

$$q = \frac{1}{4(5-6\eta_0+w(3+6\eta_0))}\left(55-76\eta_0+12\eta_0^2+9(w+2w\eta_0)^2+w\left(48+72\eta_0-48\eta_0^2\right)\right.$$
$$\left.+\sqrt{(5-6\eta_0+w(3+6\eta_0))^2\left(81-6w(3-2\eta_0)^2-28\eta_0+4\eta_0^2+9(w+2w\eta_0)^2+288\xi_0\right)}\right),$$

and

$$\Sigma^2 = \frac{1}{64(5-6\eta_0+w(3+6\eta_0))^2}\left(35-52\eta_0+12\eta_0^2+9(w+2w\eta_0)^2+w\left(36+48\eta_0-48\eta_0^2\right)\right.$$
$$\left.+\sqrt{(5-6\eta_0+w(3+6\eta_0))^2\left(81-6w(3-2\eta_0)^2-28\eta_0+4\eta_0^2+9(w+2w\eta_0)^2+288\xi_0\right)}\right)^2, \tag{51}$$

where

$$\eta_0 > \frac{3}{2}, \quad \xi_0 = 0, \quad w = \frac{1}{3}, \tag{52}$$

or

$$\eta_0 > \frac{3}{2}, \quad \frac{1}{3} < w < \frac{-5+6\eta_0}{3+6\eta_0}, \quad 0 \leq \xi_0 \leq \frac{1}{9}\left(-1+3w\right). \tag{53}$$

We will subsequently denote the region defined by (52), (53) as S2(BIMV).

Under the conditions (52), the characteristic polynomial of the dynamical system at this point is given by

$$c(\lambda) = \frac{1}{-3+2\eta_0}\left(-36\left(3+\sqrt{(-3+2\eta_0)^2}\right)-8\eta_0^3(-4+\lambda)+\left(87+28\sqrt{(-3+2\eta_0)^2}\right)\lambda-2\left(9+4\sqrt{(-3+2\eta_0)^2}\right)\lambda^2\right.$$
$$+3\lambda^3-4\eta_0^2\left(4\left(9+\sqrt{(-3+2\eta_0)^2}\right)-13\lambda+2\lambda^2\right)$$
$$\left.-2\eta_0\left(-12\left(9+2\sqrt{(-3+2\eta_0)^2}\right)+\left(59+12\sqrt{(-3+2\eta_0)^2}\right)\lambda-12\lambda^2+\lambda^3\right)\right). \tag{54}$$

Solving Eq. (54) for λ in the region described by Eq. (52), gives the eigenvalues

$$\lambda_1 = 0, \lambda_2 = -1-2\eta_0, \tag{55}$$

which shows that in this case, the equilibrium point is a local sink.

We were not able to find closed-form expressions for the eigenvalues of the dynamical system in the region defined by Eq. (53). We therefore used numerical methods to determine some eigenvalues to get a good idea as to the local behaviour of the system about this point. As can be seen from Table I, all of the computed eigenvalues in this region

TABLE I: Eigenvalues of the Dynamical System determined by numerical methods in the region defined by Eq. (53).

λ_1	λ_2	λ_3
-6.19013	-6.17073	-0.0200152
-8.19018	-8.17053	-0.0199997
-10.1902	-10.1707	-0.199906
-12.1903	-12.1708	-0.0199846
-14.1903	-14.171	-0.0199804
-16.1904	-16.1711	-0.0199773
-18.1904	-18.1713	-0.0199751
-20.1905	-20.1714	-0.0199733

are negative. There is therefore strong evidence that the equilibrium point in this region is that of a local sink.

It is of interest to note that to the authors' best knowledge at the time of the writing of this paper, the equilibrium point of our dynamical system with $\Sigma_+ \neq 0$, $\Sigma_- \neq 0$, and $\mathcal{B}_2 \neq 0$ has not been given previously in the literature in the context of a dynamical systems approach to modelling viscous magnetic fluid universes. This in turn also implies that the model will not isotropize in the regions defined by Eqs. (52) and (53).

V. BIFURCATIONS

The physical equilibria found in the previous section are related to each other by a sequence of bifurcations, which can be understood as follows. Consider the linearized equation for $\mathcal{B}_2$ at $\mathcal{F}$

$$\mathcal{B}_2' = \mathcal{B}_2 \left[\frac{1}{2} \left(-1 + 3w - 9\xi_0 \right) \right], \tag{56}$$

which destabilizes $\mathcal{F}$ at

$$\xi_0 = \frac{1}{9} \left(-1 + 3w \right). \tag{57}$$

We therefore see that the line given by Eq. (57) is very important with respect to the dynamical evolution of the system as it governs the bifurcations and transitions from one equilibrium state to the next. Interestingly, the quantity given by Eq. (57) is a boundary for the regions defined by each equilibrium point, $\mathcal{F}$ and $\mathcal{BI}_{\mathcal{MV}}$. In the case of $\mathcal{K}$, the bifurcation equation is trivially satisfied for $\xi_0 = 0$, and $w = \frac{1}{3}$ which satisfies the boundary region for $\mathcal{K}$.

For convenience, we have summarized the results of the previous section in Fig. (1) which depicts the different regions of sinks, saddles, and sources of the dynamical system.

FIG. 1: A depiction of the different regions of sinks, sources, and saddles of the dynamical system as defined by the aforementioned restrictions on the values of the expansion-normalized bulk and shear viscosities, ξ_0, η_0 and equation of state parameter, w.

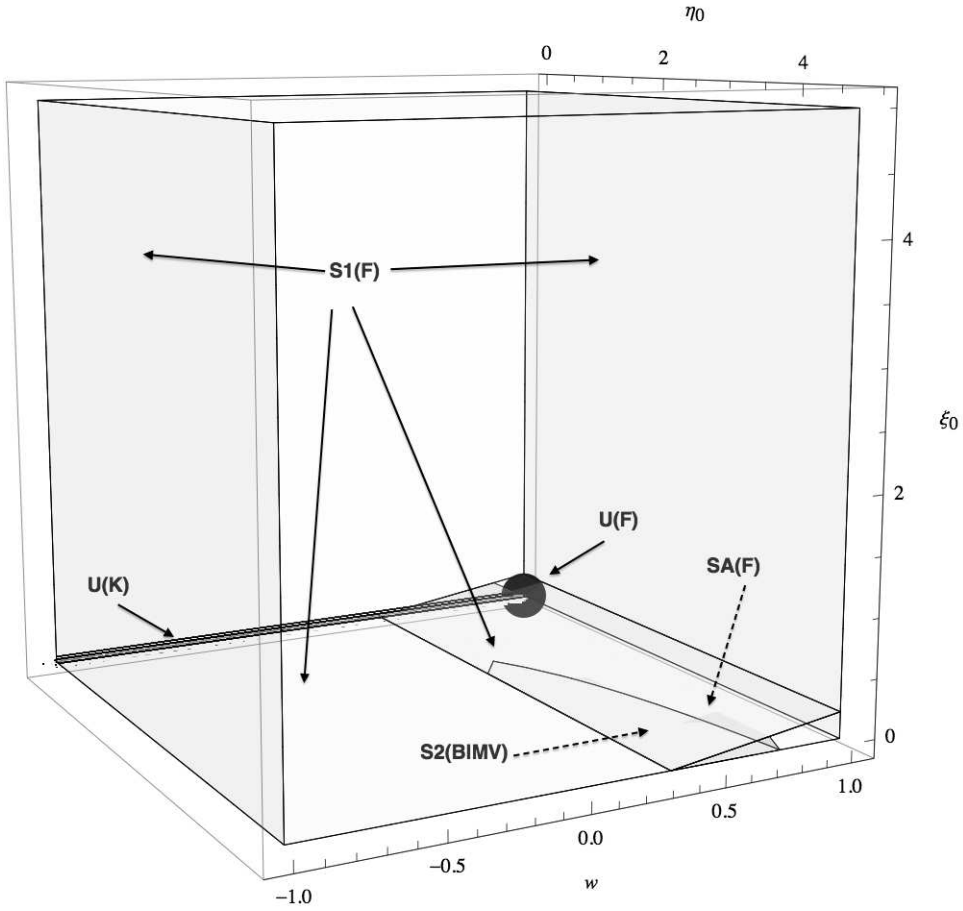

As can be seen from Fig. (1) and the above fixed-point analysis, a possible bifurcation sequence is given for when $\frac{1}{3} \leq w < 1$ is held constant, and $\eta_0 > \frac{3}{2}$. Then, we have that

$$BIMV \xrightarrow{\xi_0 \leq \frac{1}{9}(-1+3w)} BIMV \xrightarrow{\xi_0 > \frac{1}{9}(-1+3w)} S1(F).$$

Therefore, the dynamical system changes its equilibrium behaviour as the expansion-normalized bulk viscosity coefficient, ξ_0 changes, which in turn depends on the chosen value of w, in addition to the requirement that $\eta_0 > \frac{3}{2}$.

VI. QUALITATIVE PROPERTIES OF THE SYSTEM

An important question to ask in analyzing some qualitative properties of the dynamical system is whether there are any invariant sets of the dynamical system. A very useful proposition in this regard is given by Proposition 4.1 in [23], which states that for a dynamical system of type (31), if $Z : \mathbb{R}^n \to \mathbb{R}$ is a C^1 function such that $Z' = \alpha Z$, where $\alpha : \mathbb{R}^n \to \mathbb{R}$ is a continuous function, then the subsets of $\mathbb{R}^n$ defined by $Z > 0$, $Z = 0$, and $Z < 0$ are invariant sets of the flow of the system of differential equations. Looking at Eq. (27), we see that this proposition applies with $Z = \mathcal{B}_2$, so $\mathcal{B}_2 = 0$ and $\mathcal{B}_2 > 0$ are invariant sets of the system. We also note that if one sets $\eta_0 = \xi_0 = 0$ in Eq. (30), then the proposition also applies with $Z = \Omega_f$, with $\Omega_f \geq 0$, defining invariant sets of the system.

With respect to existence of limit sets and monotone functions, we first make a proposition about the late-time dynamics of the system.

Proposition 1 *Consider the dynamical system (15) in the region defined by $-1 \leq w < \frac{1}{3}$, $\xi_0 = 0$, and $\eta_0 \geq 0$. Then, as $\tau \to +\infty$, $\Sigma^2 = \Sigma_+^2 + \Sigma_-^2 \to 0$ and $\mathcal{B}_2^2 \to 0$, hence, the model isotropizes.*

Proof. The details of the proof essentially follow the arguments given in the appendix of [25]. Looking at Eq. (29), we have upon using Eq. (28) that

$$q = \Sigma^2 \left(\frac{3-3w}{2}\right) + \mathcal{B}_2^2 \left(\frac{3-9w}{4}\right) + \frac{3w+1}{2} - \frac{9}{2}\xi_0. \tag{58}$$

The Ω_f' evolution equation (30) now takes the form

$$\Omega_f' = \Omega_f \left[\Sigma^2 (3-3w) + \mathcal{B}_2^2 \left(\frac{3-9w}{2}\right) - 9\xi_0\right] + 4\eta_0\Sigma^2 + 9\xi_0. \tag{59}$$

In addition, from the generalized Friedmann equation, Eq. (28), we have that

$$\begin{aligned} \Omega_f &= 1 - \frac{3}{2}\mathcal{B}_2^2 - \Sigma^2 \\ \Rightarrow \Omega_f - 1 &= -\frac{3}{2}\mathcal{B}_2^2 - \Sigma^2 \\ \Rightarrow \Omega_f - 1 &\leq 0 \\ \Rightarrow \Omega_f &\leq 1. \end{aligned} \tag{60}$$

Therefore, to prove the proposition all we have to do is show that the function Ω_f is monotonically increasing, that is, $\Omega_f' > 0$. Since we have the freedom to choose ξ_0, we will let $\xi_0 = 0$. Then,

$$\left[\Sigma^2 (3-3w) + \mathcal{B}_2^2 \left(\frac{3-9w}{2}\right)\right] + 4\eta_0\Sigma^2 > 0 \Rightarrow -1 \leq w < \frac{1}{3}. \tag{61}$$

Therefore, in the region where $\eta_0 \geq 0$, $\xi_0 = 0$, and $-1 \leq w < \frac{1}{3}$, Ω_f is monotonically increasing. In can therefore be said that in this region,

$$\lim_{\tau \to +\infty} \Omega_f = 1. \tag{62}$$

Using this fact then in the Friedmann equation, (28), we have that

$$\lim_{\tau \to +\infty} \Omega_f = 1 \Rightarrow \lim_{\tau \to +\infty} \left(-\frac{3}{2}\mathcal{B}_2^2 - \Sigma^2\right) = 0. \tag{63}$$

The latter then implies that

$$\lim_{\tau\to+\infty}\Sigma^2=\lim_{\tau\to+\infty}\mathcal{B}_2^2=0. \tag{64}$$

To be technically correct, one should really set $\eta_0=0$. This is because we have just shown that in the region under consideration, the model isotropizes. Therefore, the isotropic universe necessarily has a perfect fluid distribution, hence $\eta_0=0$, which is still perfectly valid under our assumptions. ■

Note that, the region under consideration of the proposition is precisely one of the regions for which $S1(F)$ is a local sink, which is precisely the conclusion we reached in the proof of the proposition above.

One can also use the extended LaSalle invariance principle, that is extending the LaSalle invariance principle for negatively invariant sets to get an idea of the past asymptotic behaviour of the dynamical system. The form of the LaSalle invariance principle that we will require for this purpose is given as Proposition B.3. in [26]. Namely, consider an autonomous system of first-order differential equations $\mathbf{x}'=\mathbf{f}(\mathbf{x})$, and let $Z:\mathbb{R}^n\to\mathbb{R}$ be a C^1 function. Let $S\subset\mathbb{R}^n$ be a closed, bounded, and negatively invariant set, and $Z'(\mathbf{x})\equiv\nabla Z\cdot\mathbf{f}(\mathbf{x})\leq 0$, $\forall\ \mathbf{x}\in S$, then $\forall\ \mathbf{a}\in S$, $\alpha(\mathbf{a})\subseteq\{\mathbf{x}\in S|Z'(\mathbf{x})=0\}$.

Proposition 2 *For the dynamical system (15),* $\alpha(\mathbf{a})\subseteq\{\Omega_f=0\}$.

Proof. Clearly the set $\{\Omega_f=0\}$ is negatively invariant, closed, and bounded. Eq. (59) in the region defined by $\{\Omega_f=0\}$ reduces to $4\eta_0\Sigma^2+9\xi_0$. Clearly, this function is ≤ 0 if and only if $\eta_0=\xi_0=0$. Therefore, $\Omega_f'=0$ if $\Omega_f=\xi_0=\eta_0=0$, which is precisely the region defining the Kasner circle according to Eqs. (36) and Eqs. (39), and so $\alpha(\mathbf{a})\subseteq\{\Omega_f=0\}$. ■

Because the dynamical system (15) is a three-parameter family of autonomous ordinary differential equations, hence having complex behaviour, we were not able to provide much more of a qualitative analysis beyond what we have done so far with regards to asymptotic behaviour and the computations of the local sinks and sources. For the remainder of the paper, we therefore employ numerical techniques to study the dynamical system more thoroughly to obtain a solid understanding of the complex dynamics involved as related to the three parameters.

VII. A NUMERICAL ANALYSIS

The goal of this section is to complement the preceding stability analysis of the equilibrium points with extensive numerical experiments in order to confirm that the local results are in fact global in nature. For each numerical solution, we chose the initial conditions such that the constraint Eq.(28) in addition to $\mathcal{B}_2\geq 0$ were satisfied.

Although numerical integrations were done from $0\leq\tau\leq 3000$, for demonstration purposes we presented solutions for shorter time intervals. We completed numerical integrations of the dynamical system for physically interesting cases of w equal to 0 (dust), 0.325 (a dust/radiation mixture), and 1/3 (radiation). Also note that in the subsequent plots, asterisks denote initial conditions.

A. Dust Models: $w = 0$

1. $\xi_0 = 0.1, \eta_0 = 0.2$

FIG. 2: This figure shows the dynamical system behaviour for $\xi_0 = 0.1$, $\eta_0 = 0.2$, and $w = 0$. The diamond indicates the FLRW equilibrium point, and this numerical solution shows that it is a local sink of the dynamical system. The model also isotropizes as can be seen from the last figure, where $\Sigma_\pm, \mathcal{B}_2 \to 0$ as $\tau \to \infty$.

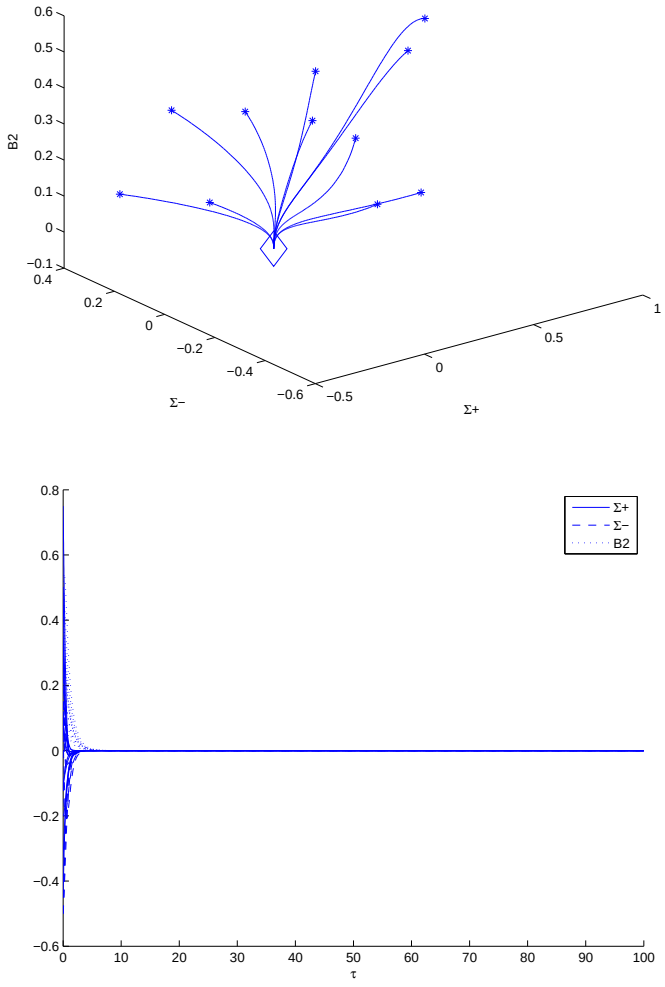

2. $\xi_0 = 1, \eta_0 = 0.5$

FIG. 3: This figure shows the dynamical system behaviour for $\xi_0 = 1$, $\eta_0 = 0.5$, and $w = 0$. The diamond indicates the FLRW equilibrium point, and this numerical solution shows that it is a local sink of the dynamical system. The model also isotropizes as can be seen from the last figure, where $\Sigma_\pm, \mathcal{B}_2 \to 0$ as $\tau \to \infty$.

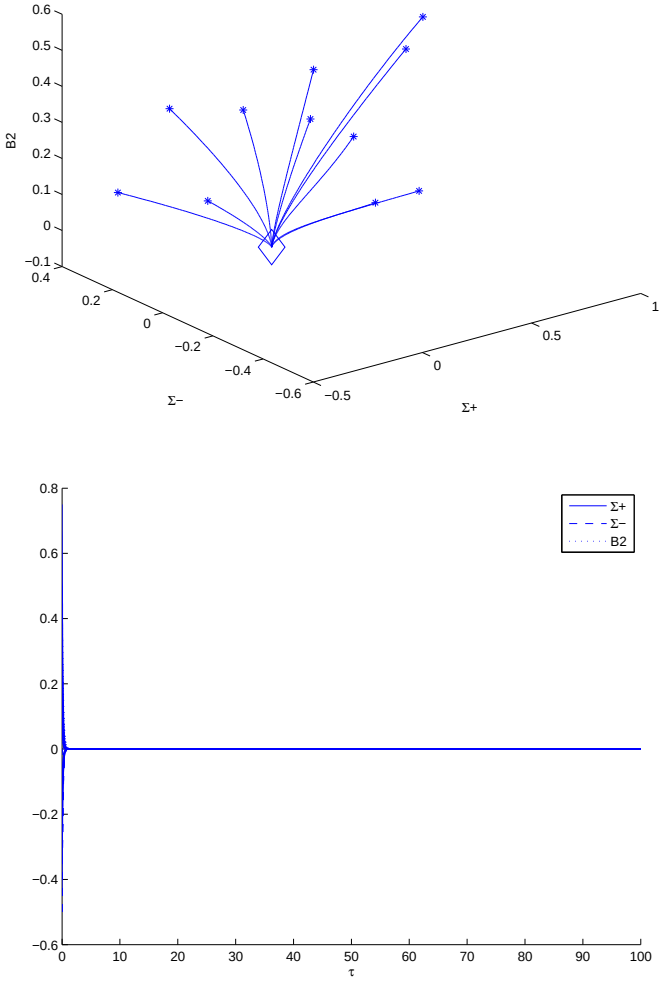

B. Radiation Models: $w = 1/3$

1. $\xi_0 = 1.5, \eta_0 = 0$

FIG. 4: This figure shows the dynamical system behaviour for $\xi_0 = 1.5$, $\eta_0 = 0$, and $w = 1/3$. The diamond indicates the FLRW equilibrium point, and this numerical solution shows that it is a local sink of the dynamical system. The model also isotropizes as can be seen from the last figure, where $\Sigma_\pm, \mathcal{B}_2 \to 0$ as $\tau \to \infty$.

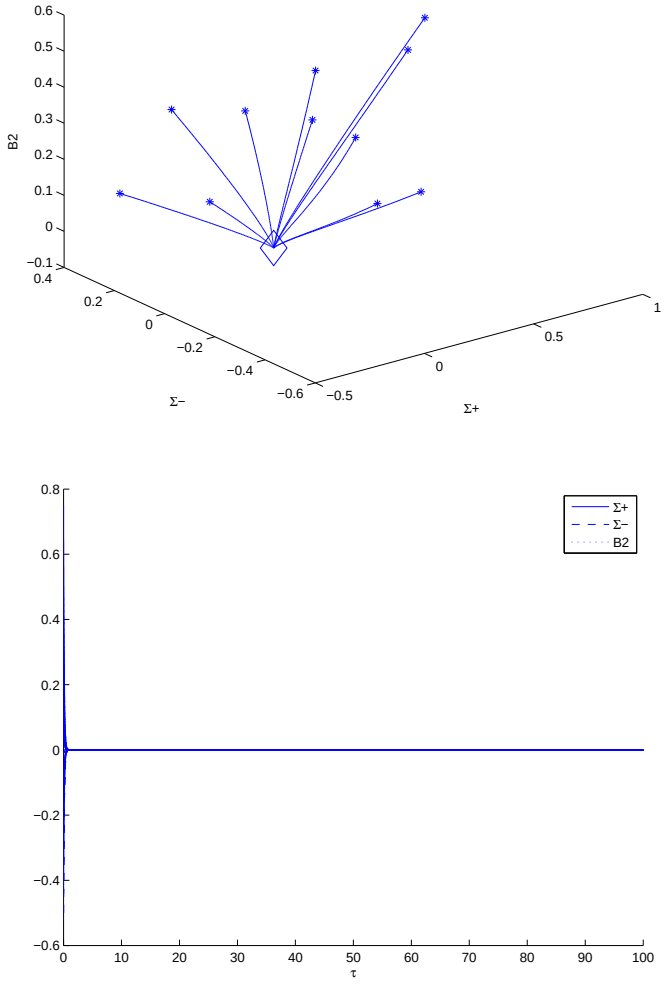

2. $\xi_0 = 1.5, \eta_0 = 0.5$

FIG. 5: This figure shows the dynamical system behaviour for $\xi_0 = 1.5$, $\eta_0 = 0.5$, and $w = 1/3$. The diamond indicates the FLRW equilibrium point, and this numerical solution shows that it is a local sink of the dynamical system. The model also isotropizes as can be seen from the last figure, where $\Sigma_\pm, \mathcal{B}_2 \to 0$ as $\tau \to \infty$.

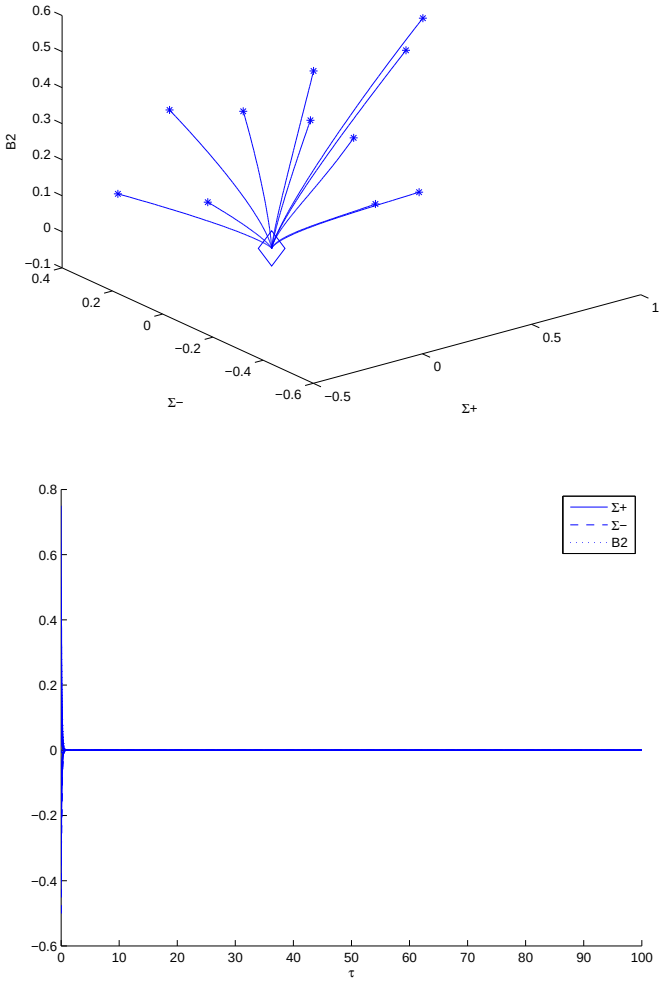

3. $\xi_0 = 0, \eta_0 = 2$

FIG. 6: This figure shows the dynamical system behaviour for $\xi_0 = 0$, $\eta_0 = 2$, and $w = 1/3$. The circle indicates the BIMV equilibrium point, and this numerical solution shows that it is a local sink of the dynamical system. The model does not isotropize with respect to the anisotropic magnetic field as can be seen from the last figure, where $B_2 > 0$ as $\tau \to \infty$, but does isotropize with respect to the spatial anisotropic variables, $\Sigma_\pm, \to 0$ as $\tau \to \infty$. This state is also special, since according to our fixed-point analysis, this behaviour is only exhibited for $w = 1/3, \eta_0 > 3/2$, and $\xi_0 = 0$

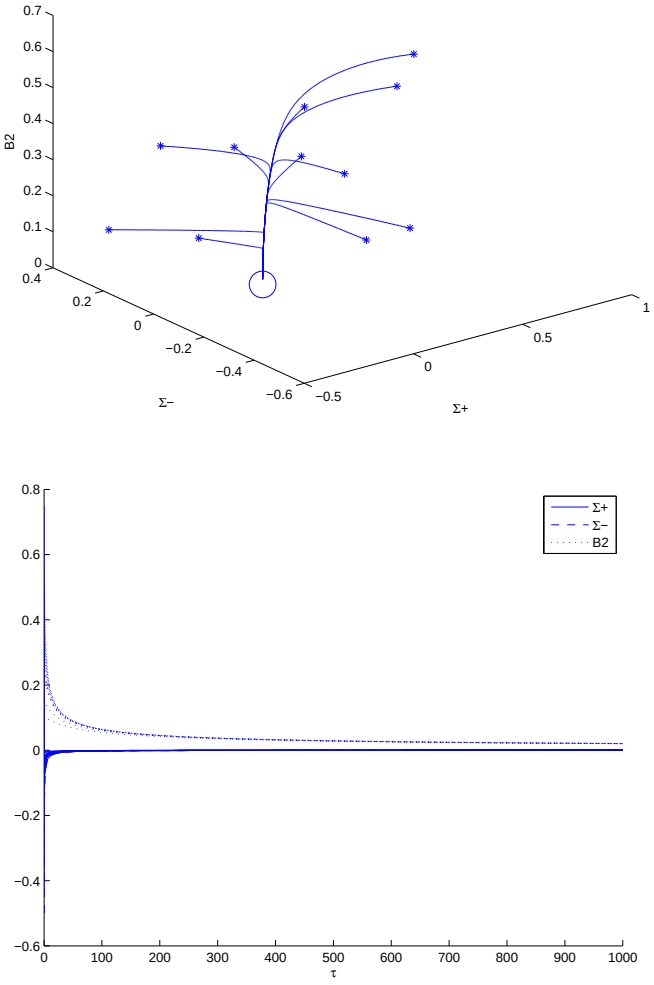

4. $\xi_0 = 0, \eta_0 = 10$

FIG. 7: This figure shows the dynamical system behaviour for $\xi_0 = 0$, $\eta_0 = 10$, and $w = 1/3$. The circle indicates the BIMV equilibrium point, and this numerical solution shows that it is a local sink of the dynamical system. The model does not isotropize with respect to the anisotropic magnetic field as can be seen from the last figure, where $B_2 > 0$ as $\tau \to \infty$, but does isotropize with respect to the spatial anisotropic variables, $\Sigma_\pm, \to 0$ as $\tau \to \infty$. This state is also special, since according to our fixed-point analysis, this behaviour is only exhibited for $w = 1/3, \eta_0 > 3/2$, and $\xi_0 = 0$

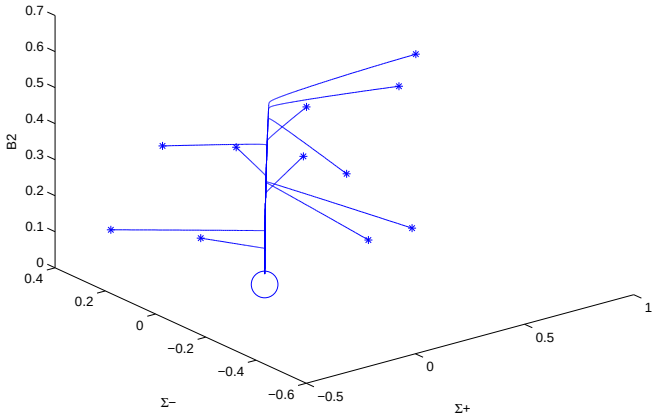

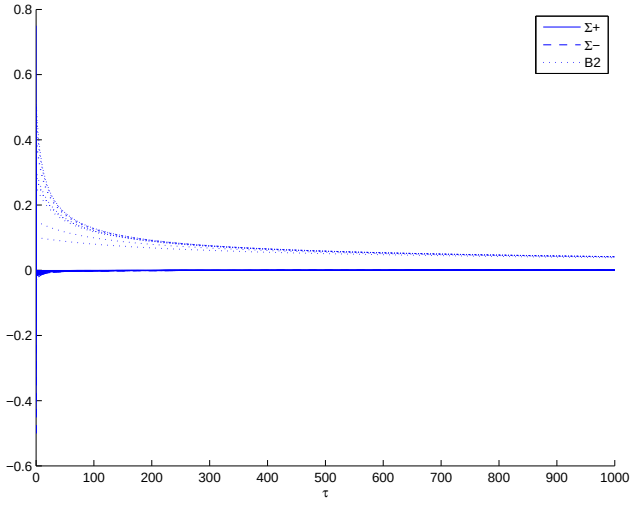

C. Dust/Radiation Models: $w = 0.325$

1. $\xi_0 = 0.5, \eta_0 = 0.5$

FIG. 8: This figure shows the dynamical system behaviour for $\xi_0 = 0.5$, $\eta_0 = 0.5$, and $w = 0.325$. The diamond indicates the FLRW equilibrium point, and this numerical solution shows that it is a local sink of the dynamical system. The model also isotropizes as can be seen from the last figure, where $\Sigma_\pm, \mathcal{B}_2 \to 0$ as $\tau \to \infty$.

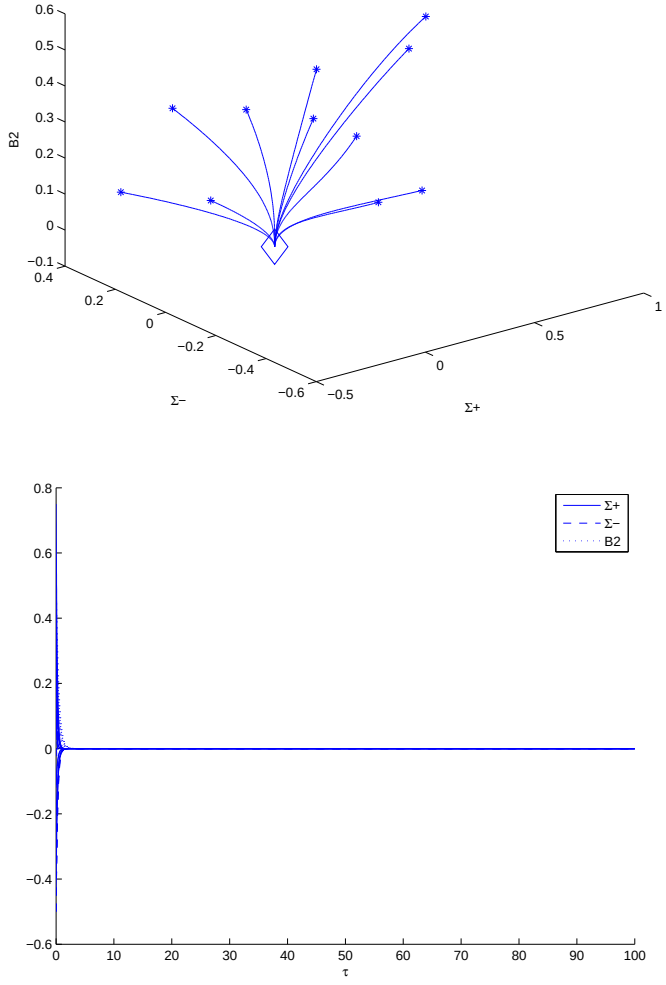

D. Dust/Radiation Models: $w = 0.325$

1. $\xi_0 = 1, \eta_0 = 2$

FIG. 9: This figure shows the dynamical system behaviour for $\xi_0 = 1$, $\eta_0 = 2$, and $w = 0.325$. The diamond indicates the FLRW equilibrium point, and this numerical solution shows that it is a local sink of the dynamical system. The model also isotropizes as can be seen from the last figure, where $\Sigma_\pm, \mathcal{B}_2 \to 0$ as $\tau \to \infty$.

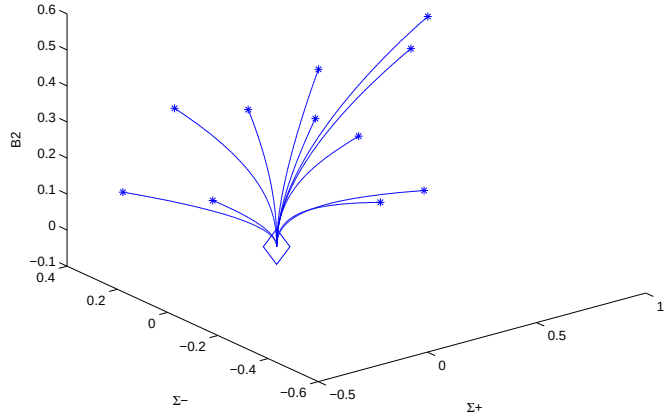

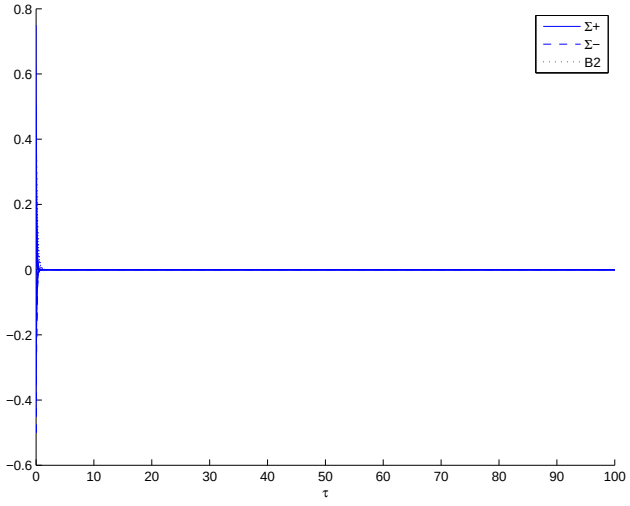

E. Bifurcations

As we alluded to previously, according to Eq. (57), the line $\xi_0 = \frac{1}{9}(-1+3w)$ governs bifurcations of the dynamical system. We therefore thought it would be constructive to display this bifurcation behaviour for cases where first $\xi_0 < \frac{1}{9}(-1+3w)$, then $\xi_0 = \frac{1}{9}(-1+3w)$, and finally, $\xi_0 > \frac{1}{9}(-1+3w)$. For the purposes of this numerical experiment, we specifically chose $w = 1/2$, $\eta_0 = 5$, therefore requiring that the three aforementioned cases reduce to $\xi_0 < \frac{1}{18}$, $\xi_0 = \frac{1}{18}$, and $\xi_0 > \frac{1}{18}$.

FIG. 10: These figures show bifurcation behaviour for a varying expansion-normalized bulk viscosity coefficient, ξ_0, while w and η_0 were held fixed. The circles indicate BIMV equilibrium points, while the diamond indicates the FLRW equilibrium point. For the first figure, $\xi_0 = 0.05$, for the second figure, $\xi_0 = \frac{1}{18}$, and for the last figure, $\xi_0 = 0.6$. Note how the increasing values of ξ_0 first result in a slight shift of the equilibrium point position of BIMV, and then finally a transition to a new state, namely the FLRW equilibrium, which was predicted by our fixed-point analysis.

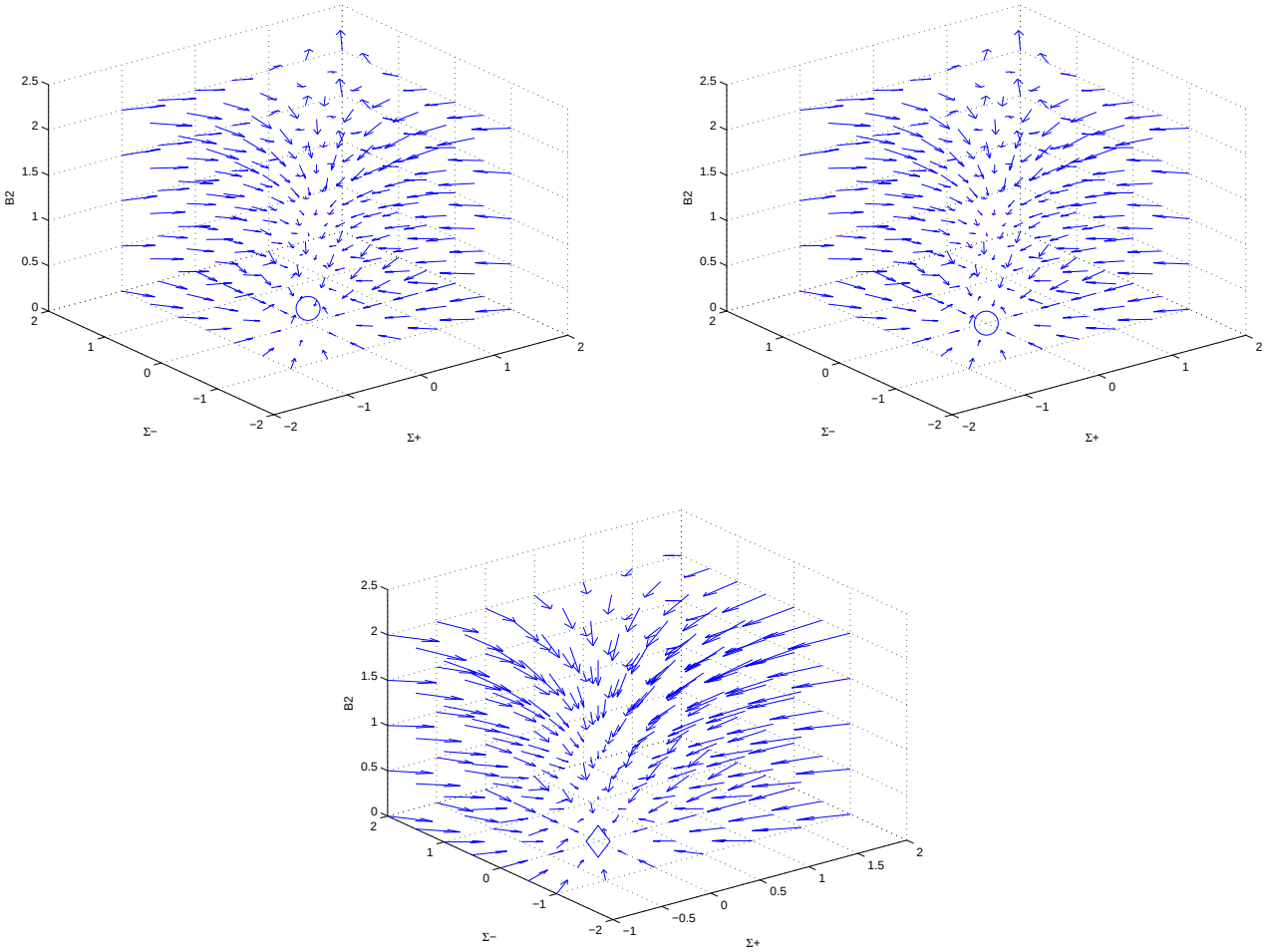

VIII. CONCLUSIONS

We have presented in this paper a comprehensive analysis of the dynamical behaviour of a Bianchi Type I viscous magnetohydrodynamic cosmology, using a variety of techniques ranging from a fixed point analysis to analyzing asymptotic behaviour using standard dynamical systems theory combined with numerical experiments. We were able to show that for cases in which $\eta_0 \geq 0, \quad \xi_0 \geq 0, \quad -1 \leq w < \frac{1}{3}$ or $\eta_0 \geq 0, \quad \frac{1}{3} \leq w \leq 1, \quad \xi_0 > \frac{1}{9}(-1+3w)$, the dynamical model isotropizes asymptotically, that is, the spatial anisotropy and the anisotropic magnetic field decay to negligible values giving a close approximation to the present-day universe. We were also able to show that for regions in which $\eta_0 > \frac{3}{2}, \xi_0 = 0, w = \frac{1}{3}$ or $\eta_0 > \frac{3}{2}, \quad \frac{1}{3} < w < \frac{-5+6\eta_0}{3+6\eta_0}, \quad 0 \leq \xi_0 \leq \frac{1}{9}(-1+3w)$, the model does not isotropize, rather at late times goes into a stable equilibrium in which there is a non-zero magnetic field.

Further to our analysis, the flat FLRW model which was our S1(F) equilibrium point, is of primary importance with respect to observational/physical significance. Through our fixed point analysis, we showed that S1(F) represents a saddle point if $\eta_0 = 0, \quad \frac{1}{3} < w < 1, \quad 0 \leq \xi_0 < \frac{1}{9}(-1+3w)$, $\eta_0 = 0, \quad w = 1, \quad 0 < \xi_0 < \frac{2}{9}$, or $\eta_0 > 0, \quad \frac{1}{3} < w \leq 1, \quad 0 \leq \xi_0 < \frac{1}{9}(-1+3w)$, (which was denoted above by SA(F)). In these regions, S1(F) attracts along its stable manifold and repels along its unstable manifold. Therefore, some orbits will have an initial attraction to S1(F), but will eventually be repelled by it. There is therefore a time period during which the cosmological model will asymptotically isotropize, and be compatible with present-day observations of high-degree isotropy.

[1] Ø. Grøn and S. Hervik, *Einstein's General Theory of Relativity: With Modern Applications in Cosmology* (Springer, 2007), 1st ed.
[2] G. F. Ellis, R. Maartens, and M. A. MacCallum, *Relativistic Cosmology* (Cambridge University Press, 2012), 1st ed.
[3] L. P. Hughston and K. C. Jacobs, Astrophysical Journal **160**, 147 (1970).
[4] V. LeBlanc, Classical and Quantum Gravity **15**, 1607 (1998).
[5] V. LeBlanc, Classical and Quantum Gravity **14**, 2281 (1997).
[6] C. Collins, Communications in Mathematical Physics **27**, 37 (1972).
[7] V. LeBlanc, D. Kerr, and J. Wainwright, Classical and Quantum Gravity **12**, 513 (1995).
[8] J. D. Barrow, R. Maartens, and C. G. Tsagas, Physics Reports **449**, 131 (2007).
[9] W. van Leeuwen and G. Salvati, Annals of Physics **165**, 214 (1985).
[10] A. Banerjee and A. Sanyal, General Relativity and Gravitation **18**, 1251 (1986).
[11] J. Benton and B. Tupper, Physical Review D **18**, 1251 (1986).
[12] G. Salvati, E. Schelling, and W. van Leeuwen, Annals of Physics **179**, 52 (1987).
[13] A. Sanyal and M. Ribeiro, Journal of Mathematical Physics **28**, 657 (1987).
[14] W. van Leeuwenn, P. Miedema, and S. Wiersma, General Relativity and Gravitation **21**, 413 (1989).
[15] A. Pradhan and O. Pandey, International Journal of Modern Physics D **12**, 1299 (2003).
[16] A. Pradhan and S. Singh, International Journal of Modern Physics D **13**, 503 (2004).
[17] R. Bali and Anjali, Pramana-Journal of Physics **63**, 481 (2004).
[18] G. Ellis and M. MacCallum, Comm. Math. Phys **12**, 108 (1969).
[19] I. S. Kohli and M. C. Haslam, Phys. Rev. D **87**, 063006 (2013), URL `http://link.aps.org/doi/10.1103/PhysRevD.87.063006`.
[20] G. F. Ellis, *Cargese Lectures in Physics*, vol. Six (Gordon and Breach, 1973), 1st ed.
[21] C. Hewitt, R. Bridson, and J. Wainwright, General Relativity and Gravitation **33**, 65 (2001).
[22] S. Hervik, W. C. Lim, P. Sandin, and C. Uggla, Classical and Quantum Gravity **27** (2010).
[23] J. Wainwright and G. Ellis, *Dynamical Systems in Cosmology* (Cambridge University Press, 1997), 1st ed.
[24] H. van Elst and C. Uggla, Class. Quantum Grav. **14**, 2673 (1997).
[25] A. A. Coley and J. Wainwright, Class. Quantum Grav. **9**, 651 (1992).
[26] C. Hewitt and J. Wainwright, Classical and Quantum Gravity **10**, 99 (1993).